UNCERTAINTIES IN PREDICTION OF TRITIUM BREEDING IN CANDIDATE BLANKET DESIGNS DUE TO PRESENT UNCERTAINTIES IN NUCLEAR DATA BASE

M. Z. YOUSSEF and M. A. ABDOU
University of California School of Engineering and Applied Science
Department of Mechanical, Aerospace, and Nuclear Engineering
Los Angeles, California 90024

Received February 25, 1985
Accepted for Publication August 6, 1985

Estimates of the uncertainty Δ_D in predicting the achievable tritium breeding ratio (TBR) due to the uncertainties in nuclear data base are presented for several fusion blanket concepts. Specifically, the impact of the current uncertainties in measuring basic nuclear data on the calculated TBR is analyzed and discussed for four leading blanket designs that utilize different breeding materials, namely, Li_2O, 17Li-83Pb, $LiAlO_2$, and Flibe. The impact on the TBR values of various evaluations for beryllium, which is employed as a multiplier in the latter two blankets, has been studied. Estimates for Δ_D in other blanket concepts have also been assessed. Moreover, estimates have been made, based on previous studies, for the contribution to Δ_D introduced by using neutron cross-section libraries that have different group structure and weighting spectra.

Based on statistically incorporating the present cross-section uncertainties and their correlation in the analysis, the range of the uncertainty in TBR was found to be between 2 and 6% in all the concepts considered. The nonstatistical treatment for cross-section errors tends to give larger values for Δ_D. The uncertainty in TBR introduced by misrepresenting the secondary energy-angle distribution of the $^9Be(n,2n')$ cross section ranges from ~4% in the Flibe to ~2% in the $LiAlO_2$ blanket. Uncertainty up to ~15% can be encountered in the TBR evaluation in thin blankets with natural ^6Li enrichment if broad-group cross-section libraries are used. However, this uncertainty can be reduced upon using an appropriate weighting spectrum representative of the one found in these blankets type.

I. INTRODUCTION

Fuel self-sufficiency in future fusion reactors based on the deuterium-tritium cycle requires that the tritium breeding ratio (TBR) exceeds unity by a margin required to compensate for losses and radioactive decay, supply enough startup inventory for other fusion reactors, and provide holdup inventory, which accounts for the time delay between production and use as well as reserve storage.[1] The required margin is uncertain at present due to the uncertainty involved in predicting the performance characteristics of the plasma and other technology components of a future fusion reactor. On the other hand, the achievable TBR for a given blanket concept is also uncertain due to the uncertainty associated with system definition (e.g., using limiter versus divertor, nonbreeding inboard blanket in a tokamak system, etc.) and the inaccuracies in predicting the TBR. The latter includes the uncertainty associated with the geometrical modeling, calculational methods, and basic nuclear data.

The uncertainties in the required TBR value due to uncertainties in the performance parameters of various fusion reactor components are the subject of Ref. 1. In this paper, we evaluate the range of uncertainties in predicting the achievable TBR arising from the current

uncertainties in the neutron cross-section data base. The uncertainties in the TBR attributed to modeling a fusion system and to applying various transport codes are not discussed here, but they are the subject of an on-going analysis. Here, emphasis is placed on the impact of the many sources of uncertainties in nuclear data on the prediction of the TBR value in various blanket concepts. These uncertainties include those introduced in generating various cross-section libraries (e.g., processing system, weighting spectra, multigroup boundaries, etc.) in addition to the uncertainty in measuring basic nuclear data. This latter uncertainty arises from the various measuring techniques used by experimentalists and the systematic errors involved in measurements. Furthermore, correlations may exist among various cross-section uncertainties over specific energy ranges. In addition, for neutron-producing cross sections such as $(n,2n')$, $(n,inelastic)$, etc., there exist uncertainties in the secondary energy distribution (SED) and secondary angular distribution, although the integrated cross section is known to a better accuracy.

Various studies have recently been conducted to assess the impact of neutron cross-section uncertainties on various responses such as tritium breeding,[2] fissile breeding in a fusion-fission hybrid system,[3,4] heating and damage rates,[5] exposure dose rate,[6] etc. These studies were limited in their scope, however, since either a particular system was considered and the analysis was performed only for that system,[7] or no statistical treatment for the cross-section uncertainties propagation was taken into consideration and only rough estimates for cross-section uncertainties were used in the analysis over limited ranges of neutron energy.[8-12]

In the present study, rigorous analysis has been conducted to statistically incorporate the present cross-section uncertainties and their correlations to derive an estimate for the range of the uncertainty Δ_D in the TBR in four of the primary blanket concepts. Moreover, estimates for Δ_D in other designs are also provided based on extrapolation of the results for the four primary concepts. Since some of the blankets considered utilize beryllium as a neutron multiplier, a serious effort has been devoted to studying the impact of various evaluations for the beryllium cross sections on the TBR.

In Sec. II, estimates of the range of the uncertainty in the TBR value are given when various multigroup cross-section libraries and weighting spectra are used in the evaluation. This section is based on results from previous studies and is included for completeness. A description of the blankets chosen for the present study is given in Sec. III. Section IV is devoted to investigating the deviation in the TBR value, using various evaluations for the ^{9}Be$(n,2n')$ cross section. Because the SED for this reaction is presented differently in these evaluations (although the integrated cross section is the same), the results given in this section reveal to what extent the TBR varies with the present uncertainty in the SED of the ^{9}Be$(n,2n')$ cross section. Results from the cross-section sensitivity and uncertainty analyses are given in Sec. V. First, a brief theoretical background for the methodology used and a description of the calculational procedures are given in Secs. V.A and V.B, respectively, while the results from the sensitivity and the uncertainty analyses are presented in Secs. V.C and V.D, respectively. Special effort has been devoted to comparing the uncertainty analysis results to those obtained with published estimates for cross-section uncertainties where the non-statistical treatment was employed. The results of such a comparison are given in Sec. V.E. Estimates for Δ_D in other blanket concepts are given in Sec. V.F, while Sec. VI is devoted to conclusions and comments regarding nuclear data uncertainties.

II. IMPACT OF VARIOUS CROSS-SECTION LIBRARIES AND WEIGHTING SPECTRA ON TRITIUM BREEDING

Recent effort was focused on predicting the attainable TBR in various blanket concepts with several multigroup neutron cross-section libraries and with different weighting spectra used to collapse fine-group to broad-group libraries.[13,14] Discrepancy among the predicted TBRs was found to depend on the type of breeding material, blanket thickness, and the degree of ^{6}Li enrichment.

An example of the results obtained from these studies is shown in Table I, taken from Ref. 13, for a 17Li-83PB self-cooled blanket. The Monte Carlo MCNP calculation, which is based on a continuous energy cross-section library, was used as the reference. Multigroup calculations were carried out with 80-, 30-, and 21-group structure libraries. For the latter two libraries, several weighting spectra were used to construct these libraries, as shown in Table I. For the naturally enriched ^{6}Li case, using a broad-group library generated with a weighting spectrum that deviates from the actual spectrum in the blanket and has fewer groups at the low-energy range can lead to a 9 to 14% decrease in the TBR when compared to the corresponding value obtained from the MCNP calculation (compare the 30-group data with spectrum 3 to the MCNP calculation). This deviation is more pronounced as the blanket thickness gets larger; however, this discrepancy ranges from -3 to -6%, using the fine 80-group library. Obviously, this range of uncertainty in the calculated TBR is still large and is comparable to the TBR uncertainty found in the present study due to the uncertainties in the basic nuclear data combined. As pointed out in Ref. 13, and for this particular blanket, which has a low ^{6}Li content, the uncertainty arising from using broad-group libraries can be narrowed if an appropriate weighting spectrum representative of

the blanket system is used to generate these libraries provided fine enough groups are used in the high-energy range. The situation is different in blankets that have highly enriched ^{6}Li. In this case, and as shown in Table I, the discrepancy in the TBR values is within a fraction of a percent, and the predicted TBR is insensitive to the library group structure and weighting spectra.[13]

Similar conclusions were reached in Ref. 14 for blankets that utilize helium as a coolant. It was found in this study that the uncertainty in the TBR calculated with several libraries for Li_2O and liquid-lithium (naturally enriched) systems is within 4%. For the Li-Pb systems excellent agreement is obtained with the broad-group libraries as compared to the MCNP results as long as most neutrons are absorbed in the blanket by ^{6}Li (highly enriched blanket). For thin ("leaky") or low-enriched ^{6}Li blankets, however, the uncertainty in the predicted TBR is as large as 10% with various libraries.

III. BLANKET CONCEPTS CONSIDERED FOR THE ANALYSIS

The material composition and dimensions for four primary blankets considered in the present work are summarized in Table II. These blankets are the Li_2O helium-cooled blanket with primary candidate alloy (PCA) structure (Li_2O/He/PCA), the 17Li-83Pb self-cooled blanket (Li-Pb/Li-Pb/PCA), the $LiAlO_2$ water-cooled blanket and beryllium multiplier and ferritic steel (FS) structure ($LiAlO_2$/H_2O/FS/Be), and the Flibe blanket (Flibe/He/FS/Be) (Ref. 15). In Table III, the TBR from ^{6}Li(T_6), from ^{7}Li(T_7), and the total breeding ratio in these blankets are shown based on a one-dimensional poloidal axis calculational model. In this calculation, the University of Wisconsin (UW) 25-group library was used, which is based on ENDF/B-IV data (see Ref. 13), except for beryllium for which the Los Alamos National Laboratory (LANL) evaluation was employed (see Sec. IV). Note, in particular, that the contribution to the total breeding from the ^{7}Li$(n,n'\alpha)t$ reactions is generally small in the Li-Pb, $LiAlO_2$, and Flibe blankets where the neutron spectrum is lower in the high-energy range as compared to the Li_2O blanket. In addition, the Li-Pb blanket has the highest TBR value as compared to other blankets.

IV. IMPACT OF VARIOUS EVALUATIONS FOR THE ^{9}Be$(n,2n')$ CROSS SECTION ON THE TBR

For the Flibe and the $LiAlO_2$ blankets, the TBR has been calculated using three evaluations for the ^{9}Be$(n,2n')$ cross sections: the ENDF/B-IV (Be-IV), the ENDF/B-V (Be-V), and the LANL evaluation (Be-LANL). The motivation behind comparing the results is that recent studies have indicated that the beryllium $(n,2n')$ cross section currently supplemented in the ENDF/B-V is in error and results in a different neutron multiplication factor when the experimental and analytical values are compared.[16,17] The ENDF/B-IV and -V evaluations are carried out by Howerton

TABLE I

Tritium Breeding Results Obtained Using Different Group Structures and Weighting Spectra*

Lithium Enrichment (% ^{6}Li)	Blanket Thickness (cm)	Continuous Energy MCNP	Discrete Ordinates ONEDANT					
			80-Group Library	30-Group Data			21-Group Data	
				Spectrum 1[a]	Spectrum 2[b]	Spectrum 3[c]	Spectrum 1	Spectrum 2
7.42	60	0.792 (0.011)[d]	0.771	0.777	0.783	0.716	0.804	0.883
	80	0.985 (0.011)	0.948	---	0.955	0.870	---	1.051
	100	1.130 (0.011)	1.066	---	1.069	0.974	1.085	1.153
90	60	1.389 (0.009)	1.393	---	1.399	1.399	---	1.431
	80	1.512	1.508	---	1.510	1.510	---	1.532

*Table taken from Ref. 13.
[a]Calculated spectrum at blanket midpoint.
[b]The $1/E$ spectrum.
[c]The spectrum used to generate the 80-group library.
[d]Fractional standard deviation.

TABLE II

Material Composition and Dimensions for the Four Blanket Concepts Considered for the Cross-Section Sensitivity/Uncertainty Analyses

Zone	Li_2O/He/PCA		Li-Pb/Li-Pb/PCA	
	Outer Radius (m)	Composition	Outer Radius (m)	Composition
1	2.53	Plasma	1.94	Plasma
2	2.73	Vacuum	2.14	Vacuum
3	2.79	First wall: 100% PCA (6.6% dense)	2.15	First wall: 50% PCA, 50% Li-Pb (90% ^{6}Li)
4	3.21	Breeding zone: 6% PCA, 85% Li_2O (density factor, 0.8), balance helium	2.75	Breeding zone: 7.5% PCA, 92.5% Li-Pb (90% ^{6}Li)
5	3.43	Plenum zone: 100% PCA (10% dense)	3.05	Reflector: 90% PCA, 10% Li-Pb (90% ^{6}Li)
6	3.73	Shield: 100% stainless steel	3.65	Shield: 90% Fe-1422, 10% H_2O
	$LiAlO_2$/H_2O/FS/Be		Flibe/He/FS/Be	
1	1.94	Plasma	1.94	Plasma
2	2.14	Vacuum	2.14	Vacuum
3	2.19	First wall: 32% HT-9, 7% H_2O, 61% void	2.20	First wall: 11.7% HT-9
4	2.39	Blanket 1: 19.5% HT-9, 21.5% H_2O, 5% $LiAlO_2$,[b] 45% beryllium,[c] 9% void	2.40	Blanket 1: 6% HT-9, 9% Flibe,[a] 53% beryllium[d]
5	2.46	Blanket 2: 12.5% HT-9, 11.5% H_2O, 70% $LiAlO_2$,[b] 6% void	2.52	Blanket 2: 6% HT-9, 9% Flibe, 75% silicon carbide (SiC)
6	2.66	Blanket 3: 7% HT-9, 4% H_2O, 84% $LiAlO_2$,[b] 5% void	2.77	Blanket 3: 28% HT-9, 9% Flibe, 53% SiC
7	2.84	Coolant manifold: 33% HT-9, 67% H_2O	2.99	Plenum: 27% HT-9
8	3.14	Shield: 80% Fe-1422, 20% H_2O	3.29	Shield: 80% Fe-1422, 20% H_2O

[a]Flibe (natural lithium): ^{6}Li, 1.135−3 (read as 1.135×10^{-3}); ^{7}Li, 1.420−2; beryllium, 1.729−2; fluorine, 4.991−2 atom/b·cm for 100% TD.
[b]Breeder (γ-$LiAlO_2$): 87% theoretical density (TD), 90% ^{6}Li enrichment.
[c]Beryllium: 87% TD.
[d]Beryllium: 100% TD.

and Perkins,[18] while the latest evaluation for the ^{9}Be(n,2n') cross section was provided by Young and Steward[19] from LANL.

As it stands, the ENDF/B-IV and -V evaluations are the same where the time sequential reaction

$$^9\mathrm{Be}(n,n_1')^{9*}\mathrm{Be}(n_2')^{8*}\mathrm{Be}$$

is allowed to be described by up to four time sequential processes through four ^{9*}Be excitation levels of 1.68, 2.43, 6.76, and 11.28 MeV. This inherent difficulty in presenting the ^{9}Be(n,2n') cross section that carried over to the ENDF/B-V evaluation limits the presentation of the ^{9}Be(n,2n') measurements by not allowing more than four levels to describe the time sequential reactions. Recent measurements by Drake et al.[16] showed that while the integrated values of the (n,2n') reaction are in good agreement with the ENDF/B-IV evaluation at energies of 5.9, 10.1, and 14.2 MeV, the differential cross section $\sigma(E \rightarrow E', \mu)$ is not. Drake et al. indicated that from ~6 to 12 MeV the cross section for excitation of the 2.43-MeV level in ^{9*}Be is substantially lower by a factor of 2; i.e., the low-lying states in the ^{9*}Be are overemphasized in the ENDF/B-IV (and -V) evaluations. This remark has also been indicated by Purser[20] and Basu et al.[17] measurements. In the work by Basu et al., the measured values of neutron multiplication were found to be ~25% lower than the calculated values in a rectangular geometry made of beryllium and surrounding the 14-MeV neutrons. This 25% deviation is due partly to the inaccuracy of the ^{9}Be(n,2n') cross-section evaluation and partly to the inaccurate method used in analyzing the experiment.

TABLE III

TBR from $^6Li(T_6)$, from $^7Li(T_7)$, and the Total Breeding Ratio in the Four Blanket Concepts*

TBR	Li_2O/He/PCA	Li-Pb/Li-Pb/PCA	$LiAlO_2$/H_2O/FS/Be	Flibe/He/FS/Be
T_6	0.8026	1.5792	1.2489[a]	1.2808[a]
T_7	0.4253	2.640−3[b]	1.999−3[a]	1.079−2[a]
T (total)	1.2279	1.5818	1.2509[a]	1.2916[a]

*Based on one-dimensional poloidal axis calculational model; data are based on ENDF/B-IV except for beryllium.
[a]Based on the LANL evaluation for beryllium; see text.
[b]Read as 2.640×10^{-3}.

The recent and unofficial evaluation for the ^9Be cross sections carried out by Young and Stewart[19] has been updated and correctly represented the energy-angle distribution of the secondary neutrons from the $^9Be(n,2n')$ reactions. In this evaluation, the $^9Be(n,2n')$ reactions, which are binned in excitation energy of $MT = 51$ to 83, are derived to agree with the evaluation by Drake et al.[16] The $(n,2n')$ distributions are based on data for a cluster of real levels in $^{9*}Be$ near 2.43 MeV ($MT = 52$) and 32 excitation energy bins to represent the $(n,2n')$ continuum.[19] We emphasized that integrating the differential cross section $\sigma(E \rightarrow E',\mu)$ over scattering angle in Young and Stewart's evaluation yields essentially the same values for the total $^9Be(n,2n')$ cross section. It is the energy-angle correlation for the $^9Be(n,2n')$ cross section that has been improved.

The Be-IV, Be-V, and Be-LANL evaluations described above have been used in the current comparative analysis, and the results are summarized in Tables IV and V for the Flibe and $LiAlO_2$ blankets, respectively. To minimize sources of difference in the evaluated TBR, we chose to use the ENDF/B-IV data base for other materials present in these blankets. In processing the beryllium data from the Be-LANL evaluation using the AMPX module,[21] only the levels $MT = 51$ to 73 were considered (the levels $MT > 73$ occur at energies higher than the 14.1-MeV neutron source). A multiplication factor of 2 is used in processing the $^9Be(n,2n')$ cross section from these inelastic levels.

Using the Be-LANL evaluation, an ~4.6% decrease in TBR from ^6Li, T_6, and a corresponding decrease of ~7.5% in T_7 are obtained in the Flibe blanket as compared to the results obtained with the Be-V evaluation. In the $LiAlO_2$ blanket, the corresponding decreases in T_6 and T_7 are 1.1 and 2.5%, respectively. However, since the tritium breeding is mostly from ^6Li, the overall decreases in the TBR are ~4.6 and 1.1% in the Flibe and the $LiAlO_2$ blankets, respectively. Also note from Tables IV and V that the contribution to the overall decrease in the TBR is mainly from the front zone of the breeding region (blanket 1) in both blankets. Simultaneous decrease in both T_6 and T_7, using the Be-LANL evaluation, can only be explained by the decrease in the number of

TABLE IV

TBR in the Flibe/He/FS/Be Blanket Using Three Different Evaluations for the Beryllium Cross Sections

Parameter	Be-V Evaluation	Be-LANL Evaluation	Decrease (%)	Be-IV Evaluation
TBR for $^6Li,T_6$				
Blanket 1 zone	9.896−1[a]	9.382−1	5.19	9.704−1
Blanket 2 zone	2.223−1	2.146−1	3.46	2.242−1
Blanket 3 zone	1.296−1	1.280−1	1.23	1.349−1
Subtotal	1.342	1.281	4.55	1.330
TBR for $^7Li,T_7$				
Blanket 1 zone	9.865−3	9.068−3	8.08	9.877−3
Blanket 2 zone	1.351−3	1.290−3	4.52	1.380−3
Blanket 3 zone	4.486−4	4.347−4	3.10	4.596−4
Subtotal	1.166−2	1.079−2	7.46	1.172−2
Total TBR	1.354	1.292	4.58	1.342

[a]Read as 9.896×10^{-1}.

TABLE V

TBR in the $LiAlO_2/H_2O$/FS/Be Blanket Using Three Different Evaluations for the Beryllium Cross Sections

Parameter	Be-V Evaluation	Be-LANL Evaluation	Decrease (%)	Be-IV Evaluation
TBR for $^6Li,T_6$				
Blanket 1 zone	1.039	1.021	1.73	1.031
Blanket 2 zone	1.427−1[a]	1.451−1	−1.68	1.489−1
Blanket 3 zone	8.125−2	8.330−2	−2.52	8.559−2
Subtotal	1.263	1.249	1.11	1.265
TBR for $^7Li,T_7$				
Blanket 1 zone	6.410−4	6.132−4	4.34	6.413−4
Blanket 2 zone	7.353−4	7.202−4	2.05	7.467−4
Blanket 3 zone	6.737−4	6.662−4	1.11	6.864−4
Subtotal	2.050−3	1.999−3	2.49	2.074−3
Total TBR	1.265	1.251	1.11	1.267

[a]Read as 1.427×10^{-1}.

neutrons available for breeding. This becomes apparent when the neutron balance in the blanket with the two evaluations is examined. We have carried out this task for both the Flibe and the $LiAlO_2$ blankets using the three evaluations. For the Flibe blanket, for example, the following conclusions are drawn:

1. Neutron multiplication is 2.02, 1.93, and 2.02, with the Be-V, Be-LANL, and Be-IV evaluations, respectively. This multiplication is solely due to the $(n,2n')$ reactions, which are dominated by the contribution from the $^9Be(n,2n')$ reaction. This contribution is ~46.4, 44, and 46.3% in the three cases, respectively.

2. Most of the neutron absorption reactions are in ^6Li. The fractions of the available neutrons contributing to T_6 are ~63.3, 63, and 62.7% in the Be-V, Be-LANL, and Be-IV cases, respectively.

3. The results from the Be-IV evaluation case are essentially the same as the Be-V evaluation case, since the $^9Be(n,2n')$ cross section is derived in the same manner in both evaluations, and are essentially based on the same data and format.

4. The decrease in the $^9Be(n,2n')$ reaction rate using the Be-LANL evaluation is ~9.3 as compared to the $^9Be(n,2n')$ reaction rate with the Be-V evaluation. However, the decrease in the neutron multiplication is ~4.3%, which is basically the same amount of decrease in the TBR. The last two conclusions emphasize that the present $^9Be(n,2n')$ evaluation in the ENDF/B-V overestimates the neutron multiplication. The ~9.3% decrease observed in the $^9Be(n,2n')$ reaction rate is due to the difference in the representation of the energy-angle distribution of the secondary neutrons obtained from this reaction rather than from the integrated value for the $^9Be(n,2n')$ cross section. In the neutron multiplication the ~25% overestimation observed by Basu et al.[17] is due to utilizing beryllium everywhere in their experiment.

It is interesting to explain the decrease in the neutron multiplication although the total $^9Be(n,2n')$ cross section is almost the same in the three evaluations. The energy-angle correlation corrected in the LANL evaluation for the secondary neutrons tends to transport these neutrons in the forward direction and away from the breeding zone (note that isotropic scattering for the second neutron in the time sequential reaction was assumed in the ENDF/B-IV and -V evaluations). Since the $^9Be(n,2n')$ reactions contribute the most to the excess neutrons, the relative amount of neutrons available for further multiplication in the beryllium zone through successive $Be(n,2n')$ reactions decreases, particularly when we note that the threshold for the $^9Be(n,2n')$ reaction is only ~2.4 MeV. Consequently, the total number of neutrons available for breeding decreases and that results in a comparable decrease in the TBR.

We have focused in the above discussion on the impact of various representations for the secondary energy and angular distribution of the $^9Be(n,2n')$ cross section on the TBR in the Flibe and the $LiAlO_2$ blankets. We would expect that the uncertainty in the TBR gets larger when the uncertainties in the secondary energy-angle distribution of similar reactions [e.g., $(n,inelastic)$, $(n,3n')$, etc.] and in other materials are considered. The example given above for the $^9Be(n,2n')$ reaction is based on *direct* evaluation for the uncertainty in the TBR due to the uncertainty in the secondary neutrons distributions. In addition to this uncertainty, there is another contribution that comes from the uncertainty in the integrated values for the various partial cross sections. This part is evaluated in Sec. V.

V. CROSS-SECTION SENSITIVITY AND UNCERTAINTY ANALYSES PROCEDURES AND RESULTS

V.A. Theoretical Background

The statistical variance in the integrated tritium production rate, $R_k \equiv \text{TBR}$, is given by[3,7,22]

$$\left(\frac{\Delta R_k}{R_k}\right)^2 = \sum_{g,g'} P_{\Sigma_x}^{g,k} P_{\Sigma_y}^{g',k} corr(\Sigma_x^g, \Sigma_y^{g'}) \times \text{RSD}(\Sigma_x^g)\text{RSD}(\Sigma_y^{g'}) \ , \quad (1)$$

where

Σ_x^g = neutron interaction cross-section type x in energy group g

$corr(\Sigma_x^g, \Sigma_y^{g'})$ = correlation matrix for the multigroup cross sections Σ_x^g and $\Sigma_y^{g'}$

$P_{\Sigma_x}^{g,k}$ = relative cross-section sensitivity profile coefficient of the response R_k due to variation in the cross-section type Σ_x^g at energy group g, and is defined as the fractional change (in percent) in the response R_k due to a 1% increase in cross section Σ_x^g at neutron group g.

The coefficient $P_{\Sigma_x}^{g,k}$ is system dependent, and its evaluation is straightforward using first-order perturbation theory,[23,24] and is given by

$$P_{\Sigma_x}^{g,k} = \frac{\delta R_k / R_k}{\delta \Sigma_x^g / \Sigma_x^g} = -\frac{1}{R_k} \langle \phi_k^*, L_{\Sigma_x} \phi \rangle_g \ , \quad (2)$$

where

ϕ, ϕ_k^* = forward and adjoint angular flux, respectively

L_{Σ_x} = portion of the Boltzmann transport operator L, which contains the cross section Σ_x.

In Eq. (2), only the indirect effect of the perturbed cross section is accounted for. If the response is also evaluated directly from Σ_x, a contribution to $P_{\Sigma_x}^{g,k}$ should be added.

The correlation matrix $corr(\Sigma_x^g, \Sigma_y^{g'})$ represents the correlation between the multigroup cross sections Σ_x^g and $\Sigma_y^{g'}$, and its elements are independent of the specific blanket under consideration. The RSD (Σ_x^g) in Eq. (1) is the relative standard deviation (RSD) of cross section Σ_x^g, and the information required to construct the correlation matrices and the RSDs for various cross-section types is implemented in file 33 of the ENDF/B-V basic data file.[25]

The relative variance in the response R_k given by Eq. (1) is made up of contributions from each material present in a particular blanket. In the uncertainty analysis results given in Sec. V.C, we assume that the uncertainty associated with cross sections of a particular material is uncorrelated to the uncertainties in the cross sections of other materials. Thus, $(\Delta R_k/R_k)^2$, given by Eq. (1), is the algebraic sum of the contributions from each material. For a particular material, however, the correlations between errors in the cross sections of that material are considered according to Eq. (1). Furthermore, and to investigate the impact of these correlations, we compare the results obtained from Eq. (1) to the case where $(\Delta R_k/R_k)^2$ is evaluated from the expression

$$(\Delta R_k/R_k)^2 = \sum_{gg'} P_{\Sigma_x}^{g,k} P_{\Sigma_y}^{g',k} corr(\Sigma_x^g, \Sigma_y^{g'}) \times \text{RSD}(\Sigma_x^g)\text{RSD}(\Sigma_y^{g'})\delta_{gg'} \ , \quad (3)$$

where $\delta_{gg'} = 1$ when $g = g'$ and zero otherwise. In this formulation, it is assumed that the correlation matrix for cross sections Σ_x^g and $\Sigma_y^{g'}$ is filled only through its diagonal, and the uncertainties are assumed to be uncorrelated between different energy groups. A more conservative evaluation for the relative variance in the response R_k can be obtained from the expression

$$(\Delta R_k/R_k)^2 = \sum_{gg'} P_{\Sigma_x}^{g,k} P_{\Sigma_y}^{g',k} \text{RSD}(\Sigma_x^g)\text{RSD}(\Sigma_y^{g'}) \ . \quad (4)$$

In Eq. (4), the uncertainties in cross sections Σ_x^g and $\Sigma_y^{g'}$ are assumed to be fully correlated over the energy range where such correlation exists (as specified in the error files of ENDF/B-V). In this case the correlation matrices are assumed to be

$$corr(\Sigma_x^g, \Sigma_y^{g'}) = \pm 1 \ , \quad (5)$$

and the sign of the correlation depends on whether Σ_x^g and $\Sigma_y^{g'}$ are correlated or anticorrelated over the specified energy range.

V.B. Calculational Procedures

To carry out the cross-section sensitivity/uncertainty analysis, the partial cross sections for each element present in each blanket were generated from the DLC41/VITAMIN-C library[26] using the AMPX module,[21] and a modified version of the SWANLAKE sensitivity code[27] was employed to generate the sensitivity profiles, values of P in a one-dimensional geometry. The integrated relative sensitivity coefficient $S_{\Sigma_x}^k$, defined as[2-12]

$$S_{\Sigma_x}^k = \sum_g P_{\Sigma_x}^{g,k} \ , \quad (6)$$

was evaluated for both responses $R_{^6\text{Li}} \equiv \text{T}_6$ and $R_{^7\text{Li}} \equiv \text{T}_7$, based on a 1% increase in the partial cross section Σ_x^g at all energy groups.

The correlation matrices and cross sections RSDs for the elements ^{6}Li, lead, iron, chromium, nickel, ^{16}O, fluorine, aluminum, silicon, carbon, hydrogen,

and beryllium were generated using the UNCER code (a modified version of the PUFF-2 code).[11] Although the results shown in Table III are based on the ENDF/B-IV evaluation (except for beryllium where the LANL evaluation is used), the generated correlations are based on the ENDF/B-V evaluation. This is not a point of concern since the correlation matrices are relative in nature.

For ^{7}Li, since only private evaluation for the ^{7}Li$(n,\alpha n')t$ cross section and its covariance exists, but has not been officially released,[28,29] the cross sections used in the calculation are those based on ENDF/B-IV. However, in carrying out the uncertainty analysis, results from the nonstatistical treatment (see Sec. V.E) were used where the ^{7}Li$(n,n'\alpha)t$ cross section was decreased by 15%. This is consistent with the new evaluation for this reaction where it was found[29] that the ^{7}Li$(n,n'\alpha)t$ cross section in the ENDF/B-IV evaluation is overestimated by ~15%. In performing the sensitivity/uncertainty analysis, the UW 25-group structure was adopted for the calculation (see Ref. 13).

V.C. Cross-Section Sensitivity Analysis Results

The relative integrated sensitivity coefficient $S^k_{\Sigma_x}$, given by Eq. (6), has been evaluated for the response $R_{T_6} \equiv T_6$ and $R_{T_7} \equiv T_7$, based on a 1% increase in the partial cross section Σ^g_x at all energies for each element present in the four blankets, and the results are summarized in Tables VI and VII for $S^{T_6}_{\Sigma_x}$ and $S^{T_7}_{\Sigma_x}$, respectively. The results shown are for those elements whose coefficients are large. From these tables, the following observations can be made.

V.C.1. Tritium Breeding from ^{6}Li, T_6

First, all reaction types that lead to neutron disappearance [e.g., (n,γ), (n,p), (n,d), $(n,t)\ldots$] have negative sensitivity coefficients as expected since these reactions decrease the number of neutrons available for tritium breeding (both from ^{6}Li and ^{7}Li). The exception is for the case of the ^{6}Li$(n,\alpha)t$ reaction, which has a positive net coefficient since the direct part, the part that comes from

$$\frac{\delta R_{6_{\mathrm{Li}}}/R_{6_{\mathrm{Li}}}}{\delta\Sigma_x/\Sigma_x} = \frac{1}{R_{T_6}}\langle\Sigma_{(n,\alpha)}\phi\rangle$$

and has a value of unity, dominates the indirect contribution evaluated from Eq. (2). As a second observation, we note that all reaction types that lead to neutron multiplication [e.g., $(n,2n')$, $(n,3n')$, $(n,2n')\alpha$] have positive coefficients since the number of neutrons available for tritium breeding increases due to these reactions.

In the Li-Pb blanket, tritium breeding from ^{6}Li is more sensitive to variations in the lead, ^{6}Li, and iron, in that order. A 1% increase in the total cross sections of these elements (equivalent to increasing the atomic densities by 1%) leads to a 0.117, 0.074, and 0.035% change in T_6, respectively. In the Li_2O blanket, however, T_6 is most sensitive to ^{7}Li, ^{6}Li, and iron, in that order, with corresponding coefficients of 0.185, 0.086, and 0.046%, respectively. Because lead is used as a neutron multiplier in the Li-Pb blanket, variation in the Pb$(n,2n')$ reaction has the largest coefficient as compared to the sensitivity coefficient for other partial reactions of other materials. The profile $P^g_{\Sigma_{(n,2n)}}$ for lead is shown in Fig. 1, and it is positive at all energies with the largest values occurring at the highest energy group.

It is interesting to note from Table VI that the (*n,inelastic*) cross section for all materials has a negative sensitivity coefficient in the Li-Pb blanket while it is positive in the Li_2O blanket. This reaction type, which occurs mainly at high energy, competes with the neutron production from the Pb$(n,2n')$ reaction in the high-energy range down to the threshold for the Pb$(n,2n')$ reaction (~7.5 MeV). In this energy range, increasing the (*n,inelastic*) reactions in the Li-Pb blanket tends to decrease the Pb$(n,2n')$ reactions, and hence the sensitivity profiles have negative values in this energy range, as shown in Fig. 2 for example. Below the Pb$(n,2n')$ threshold, however, the profiles for the (*n,inelastic*) reactions have positive values since in this case the (*n,inelastic*) reactions

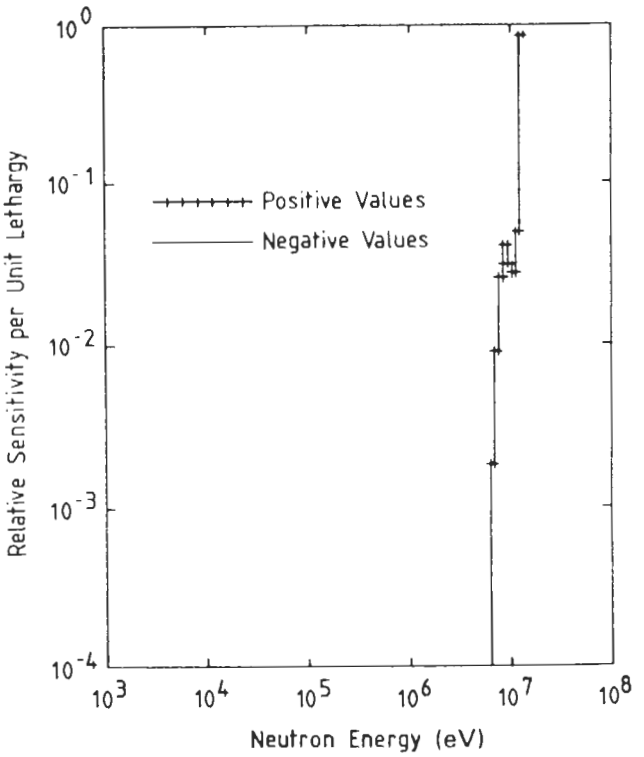

Fig. 1. The relative sensitivity profile for the Pb$(n,2n')$ cross section in the Li-Pb/Li-Pb/PCA blanket integrated over the system.

TABLE VI

Integrated Relative Sensitivity Coefficient $S_{\Sigma_x}^{T_6}$ for the TBR from ^{6}Li Due to a 1% Increase in the Various Partial Cross Sections of Materials Present in Four Blanket Concepts

Cross Section Perturbed	Li_2O/He/PCA			Li-Pb/Li-Pb/PCA			$LiAlO_2$/H_2/FS/Be			Flibe/He/FS/Be		
	^{7}Li	^{6}Li	Iron	Lead	^{6}Li	Iron	Iron	Beryllium	^{6}Li	Iron	Beryllium	^{6}Li
(*n*, *elastic*)	7.23−2[a]	4.44−3	1.46−2	4.26−2	5.20−3	1.58−2	−7.40−3	−5.24−3	2.21−3	3.29−2	1.34−1	1.09−4
(*n*, *inelastic*)	6.55−2	5.81−3	1.97−2	−1.86−2	−9.02−3	−2.24−2	−6.01−2		1.92−3	−3.62−2		−1.23−4
(*n*,2*n*′)	2.39−2		5.10−2	1.07−1		6.41−3	5.70−2	2.51−1[b]		1.65−2	4.13−1[b]	
(*n*,3*n*′)				7.33−3								
(*n*,γ)	−4.84−4	−3.49−5	−1.95−2	−2.11−2	−2.67−5	−1.63−2	−5.67−2	−4.61−4	−4.04−5	−1.74−1	−4.14−3	−3.33−5
(*n*,^{3}He)			−1.94−5			−2.46−5	−7.00−5			−3.39−5		
(*n*,*p*)			−1.46−2		−6.71−4	−1.29−2	−4.37−2	−1.87−5	−5.76−4	−2.19−2	−3.39−5	−2.71−5
(*n*,*t*)			−2.32−5			−3.01−5	−8.49−5	−6.72−3		−4.10−5	−1.24−2	
(*n*,*d*)	−6.91−3		−1.62−3			−1.83−3	−5.48−3			−2.66−3		
(*n*,*n*′*p*)			5.60−4			−1.50−3	−2.84−3			−1.83−3		
(*n*,2*n*′)α	3.20−2	6.11−3			6.69−4				1.67−3			4.04−5
(*n*,*n*′)α			4.07−5			−1.12−4	−2.14−4			−1.34−4		
(*n*,α)		7.10−2[c]	−4.13−3		7.75−2[c]	−3.97−3	−1.29−2	−3.06−2	3.89−2[c]	−6.40−3	−6.03−2	1.85−1[c]
(*n*, *absorption*)	−7.40−3	6.96−2[c]	−3.99−2	−2.11−2	7.68−2[c]	−3.51−2	−1.19−1	−3.78−2	3.83−2[c]	−2.05−1	−7.68−2	1.85−1[c]
(*n*, *total*)	1.85−1	8.60−2[c]	4.56−2	1.17−1	7.35−2[c]	−3.51−2	−1.30−1	2.08−1	4.41−2[c]	−1.92−1	4.71−1	1.85−1[c]

[a]Read 7.23×10^{-2}.
[b]Sum of contribution from each inelastic level used to represent the ^{9}Be(*n*,2*n*′) reaction in the Be-LANL evaluation.
[c]Values shown include the direct contribution to the sensitivity coefficient from perturbation in the ^{6}Li(*n*,α)*t* cross section.

TABLE VII

Integrated Relative Sensitivity Coefficient $S_{\Sigma_x}^{T_7}$ for the TBR from ^{7}Li Due to a 1% Increase in the Various Partial Cross Sections of Materials Present in Four Blanket Concepts

Cross Section Perturbed	Li_2O/He/PCA			Li-Pb/Li-Pb/PCA			$LiAlO_2$/H_2O/FS/Be			Flibe/He/FS/Be		
	^{7}Li	^{16}O	Iron	^{7}Li	Lead	Iron	^{7}Li	Iron	Beryllium	^{7}Li	Beryllium	Iron
(*n*, *elastic*)	−7.93−2[a]	−2.36−2	−6.32−4	−3.24−4	−6.30−3	−1.24−3	−3.25−3	−4.65−2	−1.52−1	−2.25−3	−5.68−2	−2.47−3
(*n*, *inelastic*)	7.07−1	−1.82−1	−8.61−2	9.99−1[b]	−1.22−1	−6.26−2	9.73−1[b]	−4.34−1		9.99−1[b]		−1.43−1
(*n*,2*n*′)	−1.83−2		−3.79−2	−1.51−4	−7.08−1	−4.35−2	−3.12−4	−1.88−1	−4.25−1[c]	−4.51−4	−4.12−1[c]	−6.58−2
(*n*,3*n*′)					−1.00−2							
(*n*,γ)	−1.10−5	−2.16−6	−2.92−5	−8.18−8	−9.04−5	−2.69−5	−2.29−7	−1.36−4	−1.12−4	−2.77−7	−1.28−4	−4.94−5
(*n*,^{3}He)			−2.01−5			−2.52−5		−1.02−4				−3.64−5
(*n*,*p*)		−1.94−2	−1.37−2			−1.34−2		−6.52−2	−3.96−5		−4.01−5	−2.30−2
(*n*,*t*)			−2.41−5		−3.09−5	−1.85−5		−1.23−4	−1.43−2		−1.47−2	−4.40−5
(*n*,*d*)	−7.68−3	−6.11−3	−1.66−3	−6.91−5		−1.89−3	−1.24−4	−8.24−3		−1.89−4		−2.88−3
(*n*,*n*′*p*)			−3.04−3			−3.65−3		−1.53−2				−5.40−3
(*n*,2*n*′)α	−2.44−2			−2.27−4			−3.86−4			−6.02−4		
(*n*,*n*′)α			−2.19−4			−2.76−4		−1.12−3				−3.97−4
(*n*,α)		−7.38−2	−4.14−3			−4.15−3		−1.98−2	−1.74−2		−2.21−2	−6.96−3
(*n*, *absorption*)	−7.70−3	−9.92−2	−1.96−2	−6.92−5	−9.04−5	−1.95−2	−1.25−4	−9.36−2	−3.19−2	−1.89−4	−3.69−2	−3.30−2
(*n*, *total*)	5.77−1[b]	−3.04−1	−1.51−1	9.98−1[b]	−8.46−1	−1.35−1	9.89−1[b]	−7.92−1	−6.09−1	9.96−1[b]	−5.06−1	−2.56−1

[a]Read 7.93×10^{-2}.
[b]Values shown include the direct contribution to the sensitivity coefficient from perturbation in the ^{7}Li(*n*,*n*′α)*t* cross section. This cross section is presented by the ^{7}Li(*n*, *inelastic*) cross section.
[c]Sum of contribution from each inelastic level used to represent the ^{9}Be(*n*,2*n*′) reaction in the Be-LANL evaluation.

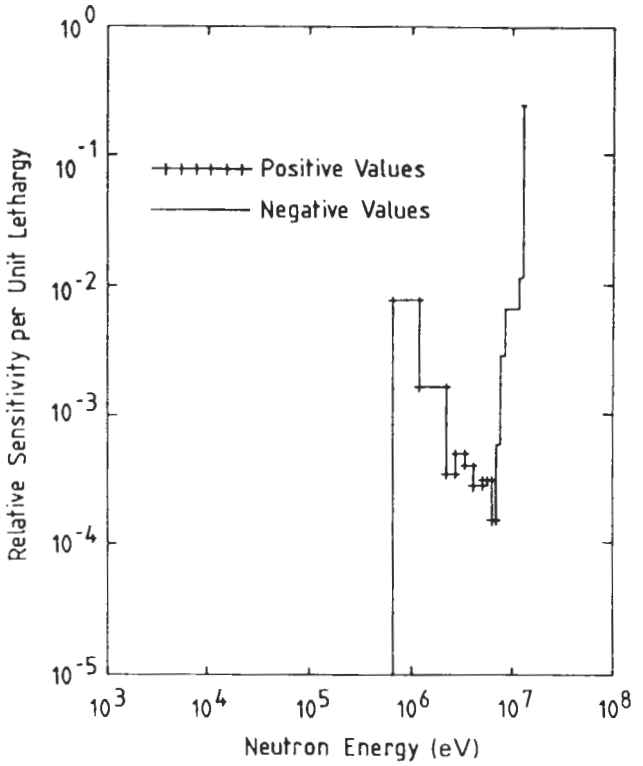

Fig. 2. The relative sensitivity profile for the Fe(*n,inelastic*) cross section in the Li-Pb/Li-Pb/PCA blanket integrated over the system.

moderate neutron energy to the range where the $^6Li(n,\alpha)t$ cross section is large and hence more breeding from ^6Li occurs. However, the net coefficient $S^{T_6}_{\Sigma_{(n,inelastic)}}$ is negative since the negative part of the sensitivity profile above the Pb($n,2n'$) threshold dominates. Since no multiplier such as lead exists in the Li_2O blanket, the profiles for the (*n,inelastic*) cross section are always positive, as shown in Fig. 3 for iron.

The (*n,elastic*) cross section has a positive coefficient for all elements in the Li-Pb and Li_2O blankets. This reaction occurs at all energies, but it is more pronounced at low energy. It tends to decrease neutron energy to the range where the $^6Li(n,\alpha)t$ cross section is large.

Note from Table VI that variations in the ^7Li cross section have practically no impact on the tritium breeding from ^6Li in the Li-Pb blanket. This is not the case in the Li_2O blanket, however, where T_6 is most sensitive to variation in the ^7Li cross section and in particular to variation in the elastic and the inelastic cross sections. In addition, the total sensitivity coefficient for ^7Li in the Li-Pb blanket is about three orders of magnitude lower as compared to the corresponding value in the Li_2O blanket. This is due to the fact that ^6Li is 90% enriched in the Li-Pb blanket, whereas natural lithium is employed in the Li_2O blanket.

The direct, indirect, and net sensitivity profiles for the $^6Li(n,\alpha)t$ cross section in the Li-Pb blanket are shown in Figs. 4 and 5. Similar profiles were obtained in the Li_2O blanket. The direct part is always positive at all energies and its profile presents the contribution to T_6 from each energy group whereas the indirect part is negative at all energies. In addition, the profiles for the $^6Li(n,\alpha)$ cross section are larger in the thermal and epithermal range in the Li_2O blanket as compared to the Li-Pb case. This is due to the fact that the neutron spectrum in the Li-Pb blanket is lower in this energy range than the corresponding spectrum in the Li_2O blanket. This is shown in Fig. 6 where the spectrum in the Li_2O blanket is about three orders of magnitude larger in the low-energy range than these values found in the Li-Pb blanket. This is true since the thermal and epithermal fluxes are depressed in the later blanket where 90% enrichment for ^6Li is used. At higher energy (>1 MeV), the Li_2O blanket exhibits larger values for the spectrum since helium is used as a coolant while the elastic and inelastic scattering processes in lead tend to soften this spectrum in the Li-Pb blanket.

The results shown in Table VI indicate that tritium breeding from ^6Li in the $LiAlO_2$ blanket is most sensitive to variations in the total cross section of beryllium, iron, and ^6Li, in that order. This is also true in the Flibe blanket with almost the same order of

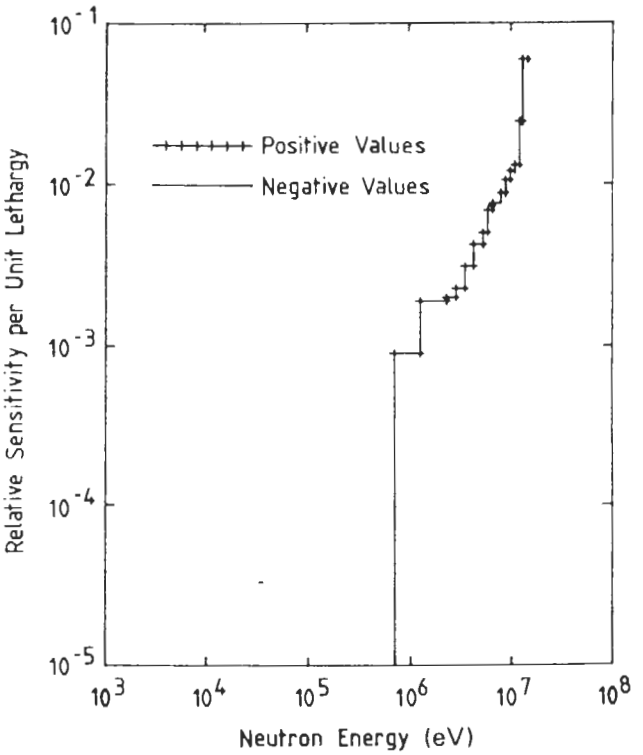

Fig. 3. The relative sensitivity profile for the Fe(*n,inelastic*) cross section in the Li_2O/He/PCA blanket integrated over the system.

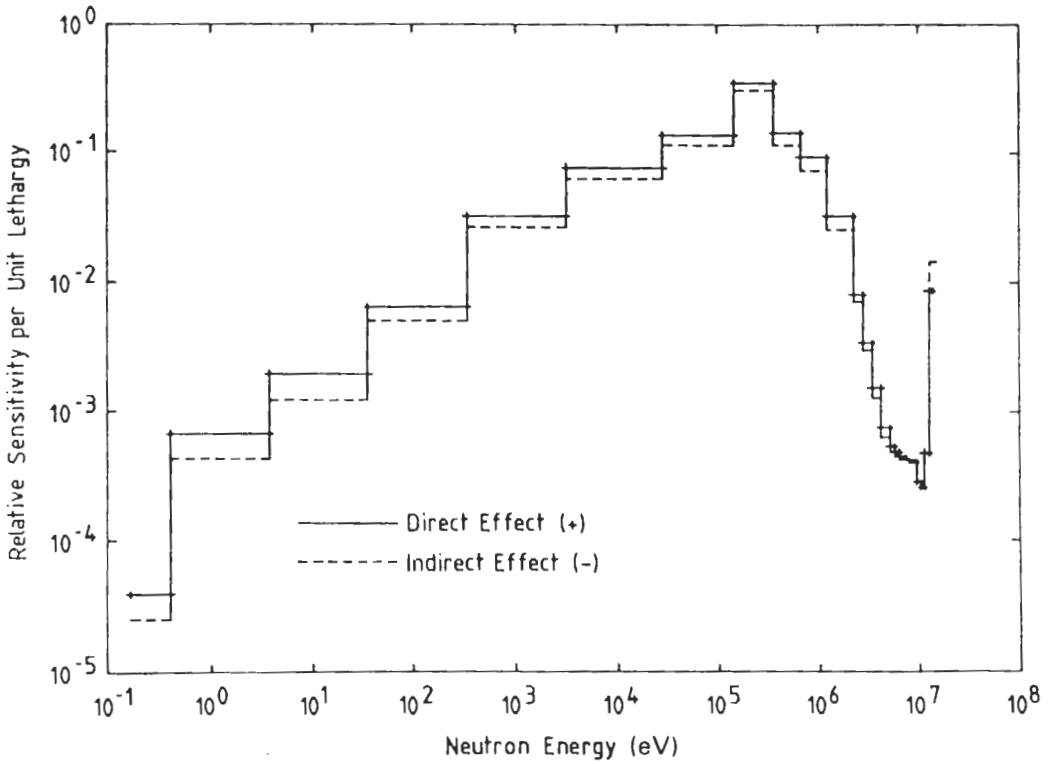

Fig. 4. The direct and indirect part of the relative sensitivity profile for the $^6Li(n,\alpha)t$ cross section in the Li-Pb/Li-Pb/PCA blanket integrated over the system.

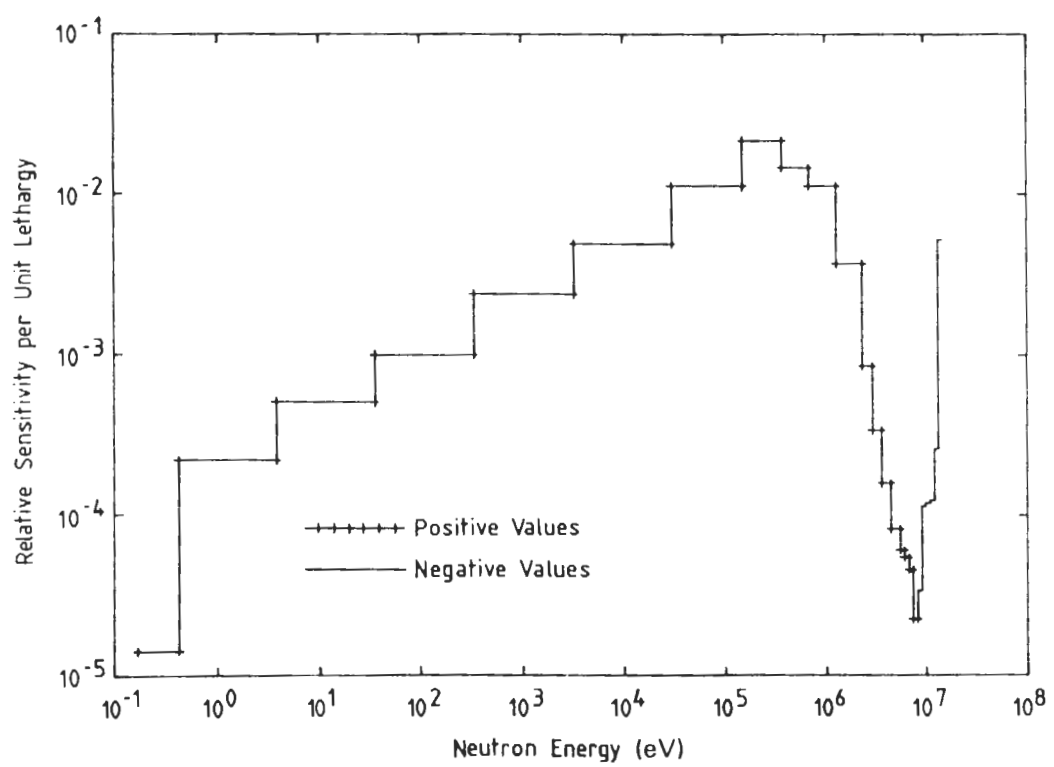

Fig. 5. The net relative sensitivity profile for the $^6Li(n,\alpha)t$ cross section in the Li-Pb/Li-Pb/PCA blanket integrated over the system.

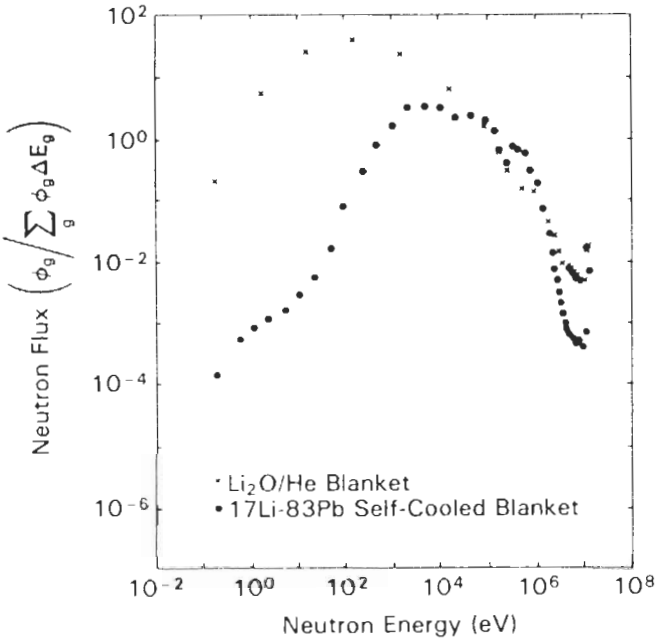

Fig. 6. The neutron spectrum in the middle of the breeding zone of the Li-Pb/Li-Pb/PCA and the Li_2O/He/PCA blankets.

magnitude for the total coefficients. Note also that increasing the structural material (equivalent to increasing the total cross section for the structure constituents) leads to a decrease in tritium production from ^{6}Li. In addition, the cross-section sensitivity coefficient to variation in the total cross section of beryllium has the largest values (0.21 and 0.47% in the $LiAlO_2$ and the Flibe blankets, respectively). As in the case for the Pb(n,2n') cross section in the Li-Pb blanket, tritium breeding from ^{6}Li has the largest sensitivity coefficient for the Be(n,2n') reactions. As cited earlier, the cross section for this reaction is constructed from the inelastic levels $MT = 51$ to 73, and the coefficient shown in Table VI for the Be(n,2n') cross section is the algebraic summation of the sensitivity coefficient for each inelastic level evaluated individually.

V.C.2. Tritium Breeding from ^{7}Li, T_7

Although tritium breeding from ^{7}Li is much smaller in the Li-Pb, $LiAlO_2$, and the Flibe blankets, as compared to the value attainable in the Li_2O blanket (see Table III), a parallel analysis was carried out to evaluate the coefficients $S_{\Sigma_x}^{T_7}$, and the results are given in Table VII.

As general observations drawn from this table, we note that all reactions leading to neutron disappearance also have negative coefficients as is the case for tritium breeding from ^{6}Li. In addition, all reactions occurring at high energy [e.g., (n,*inelastic*), (n,$n'p$), (n,2n')α, etc.] have negative coefficients since increasing these reactions is at the expense of decreasing the ^{7}Li(n,$n'\alpha$)t reaction. In fact, the total sensitivity coefficients are all negative except for the ^{7}Li(n,$n'\alpha$)t cross section (treated as the inelastic cross section in the tables shown), which has a positive coefficient, as expected. We also note that positive variations in the ^{6}Li total cross section always lead to negative coefficients in all the blankets, but the impact is practically negligible as compared to other elements. In addition, increasing the structural materials in the three blankets leads to a decrease in T_7 since they exhibit negative sensitivity coefficients. Note also that the largest coefficient is due to variation in the ^{7}Li(n,*total*) cross section, and the contribution comes mainly from the ^{7}Li(n,*inelastic*) and ^{7}Li(n,*elastic*) cross sections.

V.D. Cross-Section Uncertainty Analysis Results

To arrive at an estimate for the uncertainty associated with tritium production in the four blankets considered, the $P_{\Sigma_x}^{g,T_6}$ and $P_{\Sigma_x}^{g,T_7}$ profiles were coupled with the correlation matrices and the RSD for the various cross-section types in the manner given by Eqs. (1) through (4).

Although tritium breeding from ^{6}Li or ^{7}Li shows high sensitivity to a particular cross-section change, the uncertainty analysis can lead to different conclusions depending on the size of the current uncertainties associated with various cross-section types. As stated in Sec. V.A, the two expressions given by Eqs. (3) and (4) were used to study the impact of the correlation between cross-section uncertainties on the final results.

Examples of the RSD and the correlation matrices $corr(\Sigma_x^g, \Sigma_y^{g'})$ are shown in Figs. 7 and 8 for ^{6}Li(n,α)t ($MAT = 1303$, $MT = 105$) and Pb(n,2n') ($MAT = 1382$, $MT = 16$). The Pb(n,2n') cross section has a large RSD of ~200%. The maximum RSD in the ^{6}Li(n,α)t cross section is only ~3.6%. Also, shown in Fig. 9 is the correlation matrix for the inelastic level $MT = 52$, where the real levels in the Be-LANL evaluation for the ^{9}Be(n,2n') cross section are clustered around 2.43 MeV. The maximum RSD for this level is ~24% and occurs near the threshold. For other levels, the RSD varies between 11 and 19%.

The results for the relative variance and RSD in the breeding ratio from ^{6}Li and ^{7}Li, individually, are given in Tables VIII and IX for the four blankets. The results shown in Table VIII for the Li_2O blanket are for the case where the correlation between the cross-section uncertainties is considered according to Eq. (1). Also given in this table are the corresponding results obtained from Eqs. (3) and (4). It is clear from this table that neglecting the correlation that exists between data uncertainties gives a smaller variance in both T_6 and T_7, while assuming that the correlation is full (± 1) overestimates these variances. This holds true for the other blankets for which we only show the correlated case in Table IX.

TABLE VIII

Relative Variance and RSD in the Tritium Breeding from ^{6}Li, ^{7}Li, and the Total Breeding Ratio Due to Cross-Section Uncertainties of Various Materials in Li_2O/Helium-Cooled Blanket

Material	$(\Delta R_{^6Li}/R_{^6Li})^2$			$(\Delta R_{^7Li}/R_{^7Li})^2$		
	Correlated	Uncorrelated	Fully Correlated	Correlated	Uncorrelated	Fully Correlated
^{6}Li	2.00−2[a]	7.04−3	3.03−3	0	0	0
^{7}Li	3.61−2[b]	3.61−2[b]	3.61−2[b]	1.39+2[b]	1.39+2[b]	1.39+2[b]
Oxygen	1.03	7.75−1	2.30	4.6	3.76	5.38
Iron	2.00−1	1.41−1	2.69−1	4.63−1	2.19−1	2.32−1
Nickel	4.68−2	1.87−2	5.60−2	9.54−2	4.79−2	1.17−1
Chromium[c]	3.23−2	2.99−2	3.30−2	5.41−1	5.32−1	4.54−1
Relative variance (total)	1.37	1.01	2.72	1.45+2	1.44+2	1.45+2
RSD (%)	1.17	1.00	1.65	1.20+1	1.19+1	1.20+1
RSD in TBR (correlated case) = ±4.92%[d]						

[a]Read as 2.00×10^{-2}.
[b]Error estimates for ^{7}Li are considered uncorrelated and are obtained from the nonstatistical treatment; see text.
[c]Covariance matrices for chromium are assumed to be the same as those for iron.
[d]Based on the values of T_6 and T_7 shown in Table III.

TABLE IX

Relative Variance and RSD in the Tritium Breeding from ^{6}Li, ^{7}Li, and the Total TBR Due to Cross-Section Uncertainties of Various Materials in the Li-Pb, $LiAlO_2$, and Flibe Blanket*

Element	Li-Pb/Li-Pb/PCA		$LiAlO_2/H_2O$/FS/Be		Flibe/He/FS/Be	
	Variance in T_6	Variance in T_7	Variance in T_6	Variance in T_7	Variance in T_6	Variance in T_7
^{6}Li	8.19−2[a]	0	1.20−3	0	3.82−2	0
^{7}Li	5.43−4	2.75+2	2.92−6	2.22+2	4.84−4	2.25+2
Oxygen			7.55−2	4.13	9.25−9	1.57−11
Iron	1.19−1	1.73−1	6.94−1	1.47+1	7.99−1	1.34
Nickel	5.14−2	8.62−2	1.49−12	2.79−12	4.09−8	1.27−12
Chromium	1.13−2	8.23−2				
Fluorine					2.98−1	5.66
Silicon					7.31−2	4.75−1
Carbon					3.76−3	1.76−2
Hydrogen			1.51−3	9.89−2		
Aluminum			1.69−3	6.50−1		
Lead	1.53+1	1.59+1				
Beryllium			3.54	9.30	9.77	9.91
Total variance	1.56+1	2.41+2	4.31	2.51+2	1.10+1	2.42+2
RSD (%)	3.95	1.55+1	2.08	1.58+1	3.31	1.56+1
RSD in the total TBR (%)	±3.98		±2.1		±3.41	

*Values shown are for the "correlated uncertainties" case. The footnotes of Table VIII apply.
[a]Read as 8.19×10^{-2}.

TABLE X

Percentage Contribution from Each Blanket Constituent to the Uncertainty in Tritium Breeding from ^{6}Li, $\Delta R_{^6Li}/R_{^6Li}$, and from ^{7}Li, $\Delta R_{^7Li}/R_{^7Li}$ in the Four Blanket Concepts Considered in the Analysis

	Li_2O/He/PCA		Li-Pb/Li-Pb/PCA		$LiAlO_2$/H_2O/FS/Be		Flibe/He/FS/Be	
Element	Variance in T_6	Variance in T_7	Variance in T_6	Variance in T_7	Variance in T_6	Variance in T_7	Variance in T_6	Variance in T_7
^{6}Li	1.46	~0	5.26−1[a]	~0	2.78−2	~0	3.47−1	~0
^{7}Li	3.64	95.86	3.48−3	9.34+1	6.77−5	8.84+1	4.40−3	9.29+1
Oxygen	75.18	3.17	---	---	1.75	1.65	8.41−8	6.49−12
Iron	14.60	3.19−1	7.63−1	7.18−2	1.61+1	5.86	7.26	5.54−1
Nickel	3.42	6.58−2	3.29−1	3.58−2	3.46−11	1.11−12	3.72−7	5.25−13
Chromium	2.36	3.73−1	2.24−2	3.41−2	---	---	---	---
Fluorine	---	---	---	---	---	---	2.71	2.34
Silicon	---	---	---	---	---	---	6.65−1	1.96−1
Carbon	---	---	---	---	---	---	3.42−2	7.27−3
Hydrogen	---	---	---	---	3.50−2	3.94−2	---	---
Aluminum	---	---	---	---	3.92−2	2.59−1	---	---
Lead	---	---	9.81+1	6.59	---	---	---	---
Beryllium	---	---	---	---	8.21+1	3.71	8.80+1	4.10

[a]Read as 5.26×10^{-1}.

In the Li_2O blanket the RSDs in T_6 and T_7 are 1.2 and 12%, respectively. However, the RSD in the total TBR is ~5%. Most of the contribution to the variance in T_6 comes from the uncertainties associated with the cross sections of oxygen (75%), iron (15%), and ^{7}Li (3.6%). Note that the sensitivity analysis reveals different results where T_6 was shown to be more sensitive to variation in the ^{7}Li, ^{6}Li, and iron cross sections, in that order, and least sensitive to variation in the ^{16}O cross sections. This demonstrates that the current uncertainties in the ^{16}O cross sections are large. Most of the contribution to the variance in T_7 is from the uncertainties in the ^{7}Li cross section. This contribution is ~96%. As pointed out in Sec. V.B, no error file for ^{7}Li is currently implemented in the ENDF/B-V although nonofficial data exist. In the present analysis a reduction of ~15% in the ^{7}Li(*n,inelastic*) cross section was assumed such that the total cross section for ^{7}Li remains the same. This treatment was considered in all the results shown in Tables VIII, IX, and X.

In the Li-Pb blanket, the RSDs in T_6 and T_7 are 3.95 and 15.5%, respectively, while the RSD in the total TBR is ~3.95% since T_7 is insignificant in this case. An ~98% contribution to the variance in T_6 comes from the uncertainties associated with the lead cross section and in particular from the uncertainties in the Pb(*n*,2*n*′) and Pb(*n*,3*n*′) cross sections. The results from the uncertainty analysis are consistent with the results obtained from the sensitivity analysis.

In the $LiAlO_2$ blanket, the RSDs in T_6 and T_7 are 2.08 and 15.8%, respectively, and the RSD in the total TBR is ~2.1%. Most of the contribution to the variance in T_6 is attributed to the uncertainties associated with the beryllium cross sections and in particular in the current uncertainties in the inelastic levels (MT = 51 to 73) used to describe the ^{9}Be(*n*,2*n*′) cross section in the Be-LANL evaluation. This contribution is ~82%, while a significant contribution (~16%) is due to the uncertainties in the iron cross sections. Note in this case that the contribution from the oxygen cross-section uncertainties is only ~1.75% in contrast to the large contribution (75%) in the Li_2O blanket. This shows that results from the sensitivity/uncertainty analyses are highly system dependent. While the uncertainty in the cross section of a particular material is acceptable in one system, it may not be the case in another system. In addition, the uncertainty analysis shows that the contribution to the RSD in T_6 is most significant from the uncertainties in the ^{9}Be, iron, and ^{16}O cross section, while the sensitivity analysis reveals that T_6 is most sensitive to variations in iron, beryllium, and ^{6}Li, in that order. The uncertainties in the cross sections of iron and oxygen contribute by ~5.9 and 1.7%, respectively, to the variance in T_7.

In the Flibe blanket the RSDs in T_6 and T_7 are 3.31 and 15.6%, respectively. The TBR has an RSD of ~3.4%. As is the case in the $LiAlO_2$ blanket, most of the contribution to the variance in T_6 is due to the uncertainties associated with the ^{9}Be(*n*,*inelastic*)

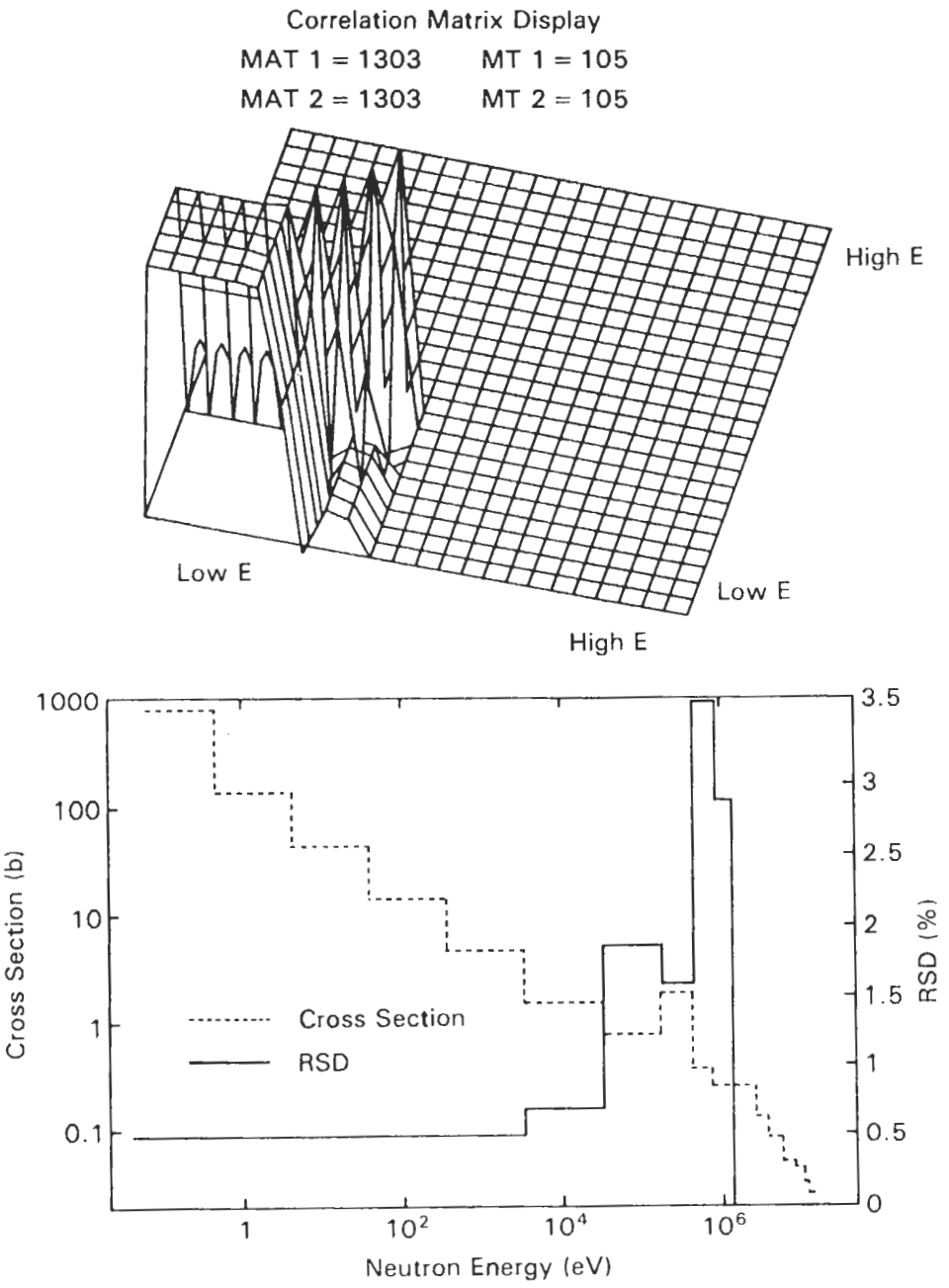

Fig. 7. The correlation matrix and RSD for the ^{6}Li ($MAT = 1303$) and reaction $(n,\alpha)t$ ($MT = 105$).

levels used to derive the ^{9}Be$(n,2n')$ cross section. Although the fluorine has a small cross-section sensitivity coefficient for T_6, the uncertainty analysis shows that the uncertainties associated with the fluorine cross sections contribute ~3% to the variance in T_6. The same uncertainties contribute ~2.3% to variance in T_7, which is again dominated by the contribution from the uncertainties in the ^{7}Li cross sections (93% contribution). A summary of the percentage contribution to the variance in T_6 and T_7 is given in Table X for the four blankets considered.

V.E. Comparison of the Uncertainty Analysis Results to Results from the Nonstatistical Treatment

The results cited in the previous sections are based on the statistical treatment for the uncertainty in the data base and its correlation characterized by the correlation matrices $corr(\Sigma_x^g, \Sigma_y^{g'})$. In previous studies,[4,10,12,30] however, the uncertainty in a response R_k was derived from the expression

$$\delta R_k / R_k = \sum_g P_{\Sigma_x}^{g,k} \cdot \frac{\delta \Sigma_x^g}{\Sigma_x^g} \quad . \tag{7}$$

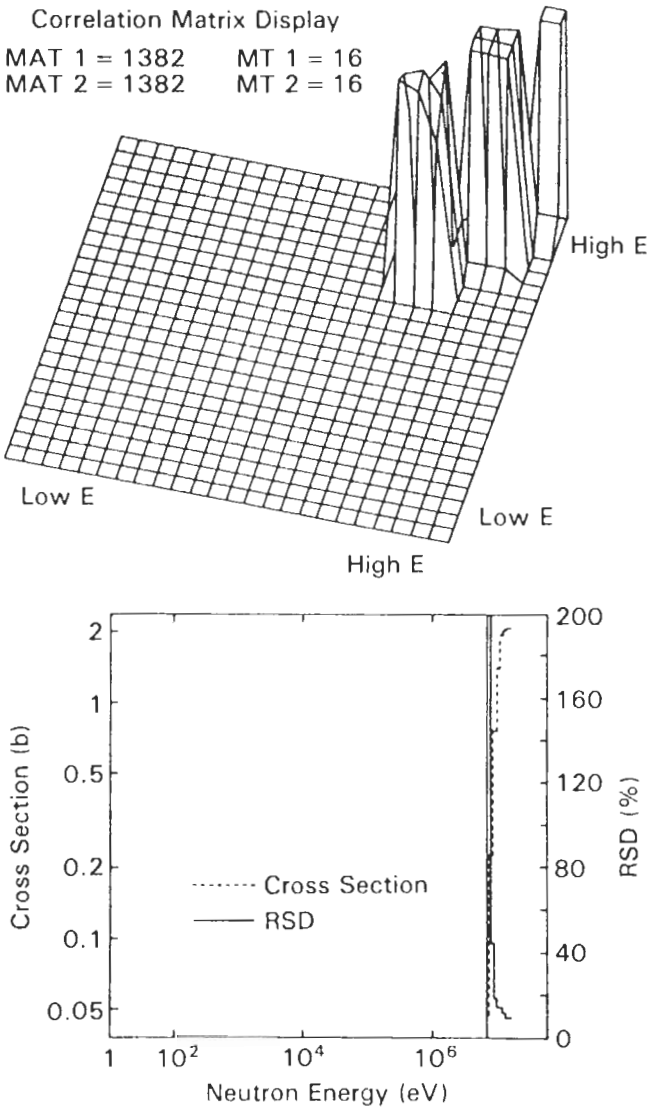

Fig. 8. The correlation matrix and RSD for the lead ($MAT = 1382$) and reaction ($n,2n'$) ($MT = 16$).

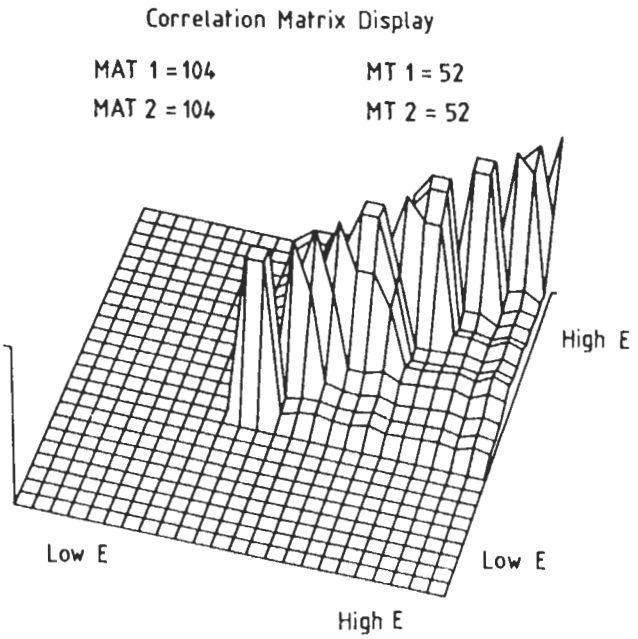

Fig. 9. The correlation matrix for beryllium ($MAT = 104$) for the inelastic level ($MT = 52$).

In Eq. (7), no correlation between the uncertainty in the cross section Σ_x^g is considered, and estimates for the relative uncertainty $\delta\Sigma_x/\Sigma_x$ are made and incorporated with the sensitivity profile according to Eq. (7). We have carried out such an analysis for the responses T_6 and T_7 in the four blankets. Some estimates for $\delta\Sigma_x/\Sigma_x$ used in this analysis are given in Table XI and are obtained from the references cited in the footnotes of that table. As stated in these studies, the total cross section is generally known to have a higher accuracy than the various partial cross sections. Therefore, it is often more realistic in specifying cross-section error in a given energy range to vary at least two partially compensating cross sections in such a manner that the total cross section remains the same. For ^{16}O we included the errors in the $^{16}O(n,total)$ cross section, and no compensating reactions were considered. For the elements ^9Be, carbon, fluorine, silicon, and aluminum, the RSD processed for each reaction type found in the ENDF/B-V error files for these elements was taken as an estimate for $\delta\Sigma_x^g/\Sigma_x^g$ and is used in Eq. (7).

The results of using this nonstatistical treatment to arrive at estimates for $\delta R_{^6Li}/R_{^6Li}$ and $\delta R_{^7Li}/R_{^7Li}$ are summarized in Table XII for the Li_2O blanket. Similar tables were obtained for other blankets (not shown). In Table XII, the contribution to the uncertainty in T_6 and T_7 from each material is given along with the values obtained from each partial and compensating cross section. Since the sensitivity profiles for the cross sections used in the analysis have different signs, error cancellation occurs. The entry "maximum $\delta R/R$" shown in this table for each element either has a positive or negative contribution to the total $\delta R/R$. If the contributions to $\delta R_{^6Li}/R_{^6Li}$ from each element are added in one direction (positive or negative) such that the change in $R_{^6Li}$ is maximum, we arrive at the value identified by the entry "$\Delta R_{^6Li}/R_{^6Li}$ (maximized to $\delta R_{^6Li}$)" shown in the table. The value for $\delta R_{^7Li}/R_{^7Li}$ in this treatment is consistent with the sign used in maximizing $\delta R_{^6Li}$. Also shown in Table XII are the corresponding values when $\delta R_{^7Li}$ is maximized. When the values for T_6 and T_7 are considered, we arrive at the expected deviation in the total TBR given in the last entry of the table for the two cases where $\delta R_{^6Li}$ and $\delta R_{^7Li}$ are maximized individually.

A comparison of the results obtained from both the statistical and nonstatistical treatment for cross-section uncertainties is shown in Table XIII. In the

TABLE XI

Error Estimates for Various Partial Cross Sections as Obtained from Literature

Element	Cross-Section Type Varied	Energy Range (MeV)	Increase in Varied Cross Section (%)	Cross-Section Type Varied to Compensate
^{6}Li[a]	$(n,\alpha)t$	$<1\times10^{-7}$	0.5	$(n,total)$
		10^{-7} to 10^{-2}	1.0	
		10^{-2} to 10^{-1}	1.0 to 2.0	$(n,elastic)$
		10^{-1} to 3×10^{-1}	5.0	
		3×10^{-1} to 5×10^{-1}	5.0 to 1.0	
		5×10^{-1} to 7×10^{-1}	10 to 15	
		7×10^{-1} to 1	15	
		1 to 1.7	15 to 10	
		1.7 to 14.1+1	10	
^{7}Li[b]	$(n,n')\alpha t$	3 to 14.1	−15	$(n,elastic)$
Lead[c]	$(n,2n')$	7.5 to 14.1	20	$(n,inelastic)$
Iron[d]	$(n,inelastic)$	8 to 15	25	$(n,elastic)$
Nickel[e]	$(n,2n')$	8 to 15	25	
Chromium[e]	$(n,n')p$	8 to 15	50	
	$(n,n')\alpha$	8 to 15	50	
	$(n,absorption)$	8 to 15	25	
^{16}O[f]	$(n,total)$	<0.5	4.0	No compensating cross sections were considered for oxygen.
		0.5 to 15	1.0	
	$(n,elastic)$	<0.5	4.0	
		0.5 to 4.0	1.0	
		4.0 to 6.5	3.0	
		6.5 to 9.5	6.0	
		9.5 to 12.5	15	
		12.5 to 15	10	
	$(n,inelastic)$	6.5 to 15	30	
	(n,γ)	All energies	14	
	(n,p)	9.5 to 15	20	
	(n,d)	9.5 to 12.5	50	
		12.5 to 15	30	
	(n,α)	2 to 15	20	

[a]Error estimates are taken from Ref. 10.
[b]Error estimates are taken from Ref. 29.
[c]Error estimates are assumed.
[d]Error estimates are taken from Ref. 5.
[e]Error estimates for nickel and chromium are considered the same as for iron. The $(n,n'\alpha)$ reaction is not considered for nickel.
[f]Error estimates are taken from Ref. 23.

statistical treatment, the uncertainty in the TBR is estimated via Eq. (1) and is introduced in the entry "errors are correlated." Neglecting the correlation that exists between the cross-section uncertainties [via Eq. (3)] gives smaller values for the uncertainty in the TBR, as shown in Table XIII. The relatively large uncertainty in the TBR value found in the Li_2O blanket is due to a combination of having a large sensitivity coefficient of T_7 to variations in the ^{7}Li cross sections [mainly $^{7}Li(n,n'\alpha)t$ cross section] and to the appreciable amount of T_7 bred in this blanket in comparison to other designs. Note that an error of −15% was assumed in the $^{7}Li(n,n'\alpha)t$ cross section used in the calculation, which is based on the ENDF/B-IV evaluation. The uncertainties cited in Table XIII should, therefore, be applied to the TBR values calculated from the ENDF/B-IV data base. On the other hand, the relatively small uncertainties in the TBR values found in the $LiAlO_2$ and Flibe blankets are due to the fact that the latest evaluation for the beryllium cross sections[19] was used. If the TBR values in these blankets were evaluated with the ENDF/B-IV (or -V) cross sections

TABLE XII

Maximum Expected Error in Tritium Breeding (Li_2O Helium-Cooled Blanket)

Element	Cross-Section Type Varied	Compensating Cross Section	$(\delta R_{^6Li}/R_{^6Li})$		$(\delta R_{^7Li}/R_{^7Li})$	
			Cross-Section Type Increased	Cross-Section Type Decreased	Cross-Section Type Increased	Cross-Section Type Decreased
^{6}Li	$(n,\alpha)t$		1.95−1[a]	−1.95−1	−2.92−2	2.92−2
		(*n, elastic*)	−3.62−2	3.62−2	5.31−2	−5.31−2
		(*n, total*)	−3.91−2	3.91−2	0.0	0.0
	Maximum $\delta R/R$		±1.20−1		±2.39−2	
^{7}Li	$(n,n'\alpha)t$		−9.82−1	9.82−1	−1.06+1	1.06+1
		(*n, elastic*)	7.92−1	−7.92−1	−1.19	1.19
	Maximum $\delta R/R$		∓1.90−1		∓1.18+1	
Oxygen	(*n, total*)	None	1.14−1	−1.14−1	−3.04−1	3.04−1
	(*n, elastic*)[b]		2.30−1	−2.3−1	−1.13−1	1.13−1
	(n,γ)		−5.47−4	5.47−4	−3.03−5	3.03−5
	(n,p)		−3.48−1	3.48−1	−3.87−1	3.87−1
	(n,d)		−1.67−1	1.67−1	−1.86−1	1.86−1
	(n,α)		−1.51	1.51	−1.48	1.48
	(*n, inelastic*)[b]		1.05	−1.05	−5.45	5.45
	Maximum $\delta R/R$		∓3.31		∓7.9	
Iron	$(n,2n')$		1.27	−1.27	−9.46−1	9.46−1
	$(n,n'\alpha)$		2.04−3	−2.04−3	−1.10−2	1.10−2
	$(n,n'p)$		2.80−2	−2.80−2	−1.52−1	1.52−1
	(*n, absorption*)		−4.66−1	4.66−1	−4.72−1	4.72−1
	(*n, inelastic*)		3.25−1	−3.25−1	−1.72	1.72
		(*n, elastic*)	−1.71−1	1.71−1	2.12−2	−2.12−2
	Maximum $\delta R/R$		±9.91−1		∓3.28	
Nickel	$(n,2n')$		9.47−2	−9.47−2	−7.03−2	7.03−2
	$(n,n'p)$		1.14−2	−1.14−2	−6.14−2	6.14−2
	(*n, absorption*)		−3.02−1	3.02−1	−3.03−1	3.03−1
	(*n, inelastic*)		7.02−2	−7.02−2	−3.72−1	3.72−1
		(*n, elastic*)	−4.22−2	4.22−2	4.89−3	−4.89−3
	Maximum $\delta R/R$		∓1.68−1		∓8.01−1	
Chromium	$(n,2n')$		2.38−1	−2.38−1	−1.76−1	1.76−1
	$(n,n'\alpha)$		2.01−4	−2.01−4	−1.17−3	1.17−3
	$(n,n'p)$		4.54−3	−4.54−3	−2.53−2	2.53−2
	(*n, absorption*)		−7.97−2	7.97−2	−8.05−2	8.05−2
	(*n, inelastic*)		4.52−2	−4.52−2	−1.72−1	1.72−1
		(*n, elastic*)	−3.51−2	3.51−2	3.71−3	−3.71−3
	Maximum $\delta R/R$		±1.73−1		∓4.51−1	
	$\delta R_i/R_i$(maximized to $\delta R_{^6Li}$)		±4.95		±16.79	
	$\delta R_i/R_i$(maximized to $\delta R_{^7Li}$)		±2.62		±24.26	
	$\left(\frac{\delta R_{Li}}{R_{Li}}\right)_{max}$ [c]		±9.05% ±10.12%			

[a]Read as 1.95×10^{-1}.
[b]Cross section varied such that maximum $\delta R/R$ is estimated.
[c]$R_{^6Li} = 0.8026$, $R_{^7Li} = 0.4253$, $R_{Li} = 1.2279$, $i = {}^6$Li or ^{7}Li.

TABLE XIII

Estimates of the Uncertainty in TBR Due to Uncertainty in Nuclear Data Base in Four Blanket Concepts

Method	Blanket Concept			
	Li_2O/He/PCA (%)	Li-Pb/Li-Pb/PCA (%)	$LiAlO_2$/H_2O/FS/Be (%)	Flibe/He/FS/Be (%)
Statistical treatment				
Errors are correlated	±4.92	±3.98	±2.1	±3.41
Errors are not correlated	±4.78	±3.80	±1.74	±2.67
Nonstatistical treatment				
$(\delta R^{6}_{Li}/R^{6}_{Li})$ maximized	±9.05	±4.70	±6.30	±7.54
$(\delta R^{7}_{Li}/R^{7}_{Li})$ maximized	±10.12	±1.49	±1.82	±4.31

for ^{9}Be, these uncertainties would be larger and a contribution from the uncertainty in the angle-energy distribution for the $^{9}Be(n,2n')$ should be added (see Sec. IV).

It is clear from this table that the statistical treatment where the covariance in the cross-section errors is considered tends to decrease the estimate for the uncertainty in the total TBR as compared to the values obtained from the nonstatistical treatment. In addition and consistent with the statistical treatment results, the Li_2O blanket exhibits the largest uncertainty in the TBR with a value of ~10%. This relatively large value is a point of concern in designing blankets that utilize Li_2O as a breeder since this blanket type has the smallest TBR value as compared to the other blankets. The larger values in the uncertainty in the TBR obtained from the nonstatistical treatment can be viewed as conservative estimates although the statistical treatment results are more realistic.

V.F. Estimates for the Uncertainty in the TBR for Other Blanket Concepts

Estimates for the uncertainty in the TBR Δ_D arising from cross-section uncertainties in other blanket concepts are summarized in Table XIV. The blanket concepts shown in this table are those rated to have more plausible features than others. The values cited are based on anticipated estimates as explained in the comments included in that table. As shown, the range of the uncertainty in the TBR due to data base uncertainties is between 2 and 6% in all the blanket concepts considered.

VI. CONCLUSIONS ON THE UNCERTAINTY IN PREDICTING THE TBR

Previous studies[13,14] have shown that the uncertainty in the TBR prediction attributed to the approximation introduced in the data with the multigroup treatment (various group structure and different weighting spectra) can be almost <1% provided that (a) high-energy neutrons are adequately treated and fine enough groups are used in the high-energy range, and (b) most neutrons are absorbed in the blanket by ^{6}Li (highly enriched systems). For thin blankets that utilize naturally enriched lithium, the discrepancy in the TBR obtained with various group structure and weighting spectrum can be as large as 4 to 15% depending on the breeding material and blanket thickness. This discrepancy can be reduced if an appropriate weighting spectrum representative of the system under consideration is used to generate broad-group libraries.

To evaluate the effect of uncertainties in the basic data arising from measurements, four blanket concepts have been considered for the cross-section sensitivity and uncertainty analysis performed in the present work. Three of these blankets utilize a neutron multiplier, lead in the Li-Pb blanket, and beryllium in both the $LiAlO_2$ and the Flibe blankets. It was found from both the sensitivity and the uncertainty analysis that the uncertainty in tritium breeding from ^{6}Li (the dominant contributor to the total breeding ratio in these three blankets) is due mainly to uncertainties associated with multiplying reactions such as the $Pb(n,2n')$, $Pb(n,3n')$, and $^{9}Be(n,2n')$ cross sections.

For the Flibe and $LiAlO_2$ blankets, and aside from the uncertainty associated with the total angle-integrated cross sections, it was found that the latest evaluation for the $^{9}Be(n,2n')$ provided by LANL results in a decrease of ~4.3% in the TBR for the Flibe blanket as compared to that obtained with the current $^{9}Be(n,2n')$ cross-section evaluation implemented in both the ENDF/B-IV and -V versions. Therefore, improving the representation of the energy-angle distribution for the secondary neutrons in a multiplying reaction can lead to a substantial change in the tritium breeding.

As shown in this study, the uncertainty analysis reveals, in some cases, different results from the sensitivity analysis. An example of such differences is

TABLE XIV

Estimate of the Uncertainty Associated with TBR $\Delta_D = \Delta T/T$ in Various Blanket Concepts Due to Uncertainties Associated with Nuclear Data Base

Number	Blanket Concept	Range of Δ_D (%)	Comments
1	Li_2O/He/PCA	~4.9	Based on extensive, detailed cross-section sensitivity/uncertainty analyses. Statistical error propagation was considered. Higher values are obtained with nonstatistical cross-section error treatment.
2	Li-Pb/Li-Pb/PCA	~3.9	See comments on blanket 1.
3	$LiAlO_2$/H_2O/FS/Be	~2.1	See comments on blanket 1.
4	Flibe/He/FS/Be	~3.4	See comments on blanket 1.
5	Li/Li/V	~6	Taken from Ref. 10. In the treatment cited in this reference, no cross-section uncertainty correlation was considered.
6	Li/Li/FS	~5.5	Assumed that the uncertainty in TBR is 0.5% less than the Li/Li/V case, since cross section for FS constituent (mainly iron, nickel) is better known than for vanadium.
7	Li/He/FS	~5	Assumed same as in the Li/Li/FS blanket, less ~0.5% due to replacing lithium by helium coolant.
8	$LiAlO_2$/He/FS/Be	~2	Assumed same as in blanket 3, less 0.1% due to the contribution from errors associated with H_2O cross section.
9	$LiAlO_2$/DS/FS/Be	~1.9	Based on normalizing the contribution to the TBR uncertainty in blanket 8 from beryllium, oxygen, aluminum, and FS to the weight of these materials in the draw salt (DS) blanket. Contributions from the DS coolant were not considered.
10	Li-Pb/Li-Pb/V	~4.4	Additional value of 0.5% was added to the uncertainty in TBR of blanket 2 for reason explained in comments on blanket 6.

the case of oxygen. While the sensitivity analysis performed on the Li_2O blanket shows that tritium breeding from ^6Li is least sensitive to variation in the oxygen cross sections, the uncertainty analysis has revealed that the current uncertainties in the oxygen cross sections lead to an ~75% contribution to the variance in T_6. In addition, the same uncertainties in oxygen cross sections contributed only ~2% to the variance in T_6 in the $LiAlO_2$ blanket. This demonstrates that the uncertainty analysis is highly system dependent.

The present uncertainties in the ^6Li cross sections seem adequate for predicting the TBR in all the blankets studied. Furthermore, no further improvement is needed in the ^7Li cross sections for blanket concepts utilizing neutron multipliers. The situation is different for blanket concepts without a neutron multiplier. For example, for the case where Li_2O is used as a breeder, the uncertainty in the $^7Li(n,n'\alpha)t$ cross section contributes ~96% to the variance in T_7 in this blanket, and almost 30% of the total breeding comes from this reaction. It has also been shown that the Li_2O blanket exhibits the largest uncertainty in tritium breeding (~5%) as compared to other blankets. As pointed out earlier, this presents a point of concern especially because the Li_2O blanket has the lowest TBR value in comparison to the achievable TBR in other blankets, and because the primary motivation for considering Li_2O as a candidate breeder is the possibility of achieving self-sufficiency without the use of a neutron multiplier. If the achievable TBR with Li_2O proves inadequate without a neutron multiplier, Li_2O will be eliminated as a candidate breeder since other breeding materials offer better chemical stability and their performance with a neutron multiplier is comparable.

Considering other blanket concepts, it seems that the uncertainty in tritium production, Δ_D, arising from the uncertainties in nuclear data base is ~2 to 6%. Our estimates for Δ_D based on statistical treatment and correlation among uncertainties give smaller values of Δ_D than those obtained from the nonstatistical treatment. The values obtained in the latter case can be considered as conservative limits.

The uncertainty evaluations given in the present work are limited for several reasons. First, perturbation theory was applied, and the results are limited by the limitation inherent in this method.[24,31,32] Second,

the uncertainty analysis results are based only on the available data regarding the uncertainty in the total angle-integrated cross sections as currently implemented in the error files of the ENDF/B-V. No error files are presently available for the uncertainty in the angle-energy distribution of the secondary neutrons emitted in neutron-producing reactions. Theories and format to incorporate the uncertainties in these secondary distributions within the perturbation theory are currently in progress.[33,34] These results from direct evaluation with a different representation for the $^{9}Be(n,2n')$ cross section emphasizes the importance of incorporating such uncertainties. Third, the sensitivity and uncertainty analyses presented in the present study are based on one-dimensional analysis. Assessment of the TBR and its uncertainty due to nuclear data in a particular conceptual reactor design that includes more design details and geometrical variation will require multidimensional cross-section sensitivity/uncertainty analyses. At present, there are computational tools to perform this task using two-dimensional transport codes.[31,35] Currently, there is an on-going effort to extend the present work to multidimensional geometries.

ACKNOWLEDGMENTS

Useful discussions with K. Shin are appreciated.

This work was supported by the U.S. Department of Energy under Contract No. DE-AM03-76SF00034.

REFERENCES

1. M. A. ABDOU et al., "Deuterium-Tritium Fuel Self-Sufficiency in Fusion Reactors," *Fusion Technol.*, **9**, 250 (1986).

2. S. PELLONI and E. T. CHENG, "Cross Section Sensitivity Study for U.S. Fusion Engineering Device (FED)," *Nucl. Technol.*, **4**, *2*, Part 3, 841 (1983).

3. M. Z. YOUSSEF et al., "Impact of Cross-Section Uncertainties on the Nuclear Design of Hybrid Reactors," *Nucl. Technol.*, **4**, 648 (1983).

4. M. Z. YOUSSEF et al., "Error Estimates of Fissile Fuel and Tritium Production in the SOLASE-H Hybrid Reactor," *Trans. Am. Nucl. Soc.*, **34**, 33 (1980).

5. R. G. ALSMILLER et al., "Uncertainties in Calculated Heating and Radiation Damage in the Toroidal Field Coil of a Tokamak Experimental Power Reactor Due to Neutron Cross-Section Errors," *Nucl. Technol.*, **34**, 376 (1977).

6. E. A. STRAKER, "Sensitivity of Secondary Gamma-Ray Dose to Angular Distribution of Gamma Rays from Neutron Inelastic Scattering," *Nucl. Sci. Eng.*, **41**, 147 (1970).

7. S. A. GERSTL et al., "Cross-Section Sensitivity and Uncertainty Analysis with Application to a Fusion Reactor," *Nucl. Sci. Eng.*, **62**, 137 (1977); see also S. A. GERSTL et al., "A Comprehensive Neutron Cross Section and Secondary Energy Distribution Uncertainty Analysis for a Fusion Reactor," LA-8333-MS, Los Alamos National Laboratory (1980).

8. Y. SEKI et al., "Macroscopic Cross-Section Sensitivity Study for Fusion Shielding Experiments," ORNL/TM-5467, Oak Ridge National Laboratory (1978).

9. Y. SEKI et al., "Comparison of One- and Two-Dimensional Cross-Section Sensitivity Calculations for a Fusion Reactor Shielding Experiment," ORNL/TM-6667, Oak Ridge National Laboratory (1979).

10. R. G. ALSMILLER et al., "Comparison of the Cross Section Sensitivity of the Tritium Breeding Ratio in Various Fusion-Reactor Blankets," *Nucl. Sci. Eng.*, **57**, 122 (1975).

11. C. R. WEISBIN et al., "Application of FORSS Sensitivity and Uncertainty Methodology to Fast Reactor Benchmark Analysis," ORNL/TM-5563, Oak Ridge National Laboratory (1976).

12. D. E. BARTINE et al., "Cross Section Sensitivity of Breeding Ratio in a Fusion Reactor Blanket," *Nucl. Sci. Eng.*, **53**, 304 (1974).

13. J. H. HUANG and M. E. SAWAN, "Tritium Breeding Benchmark Calculations for a $Li_{17}Pb_{83}$ Blanket with Steel Structure," *Fusion Technol.*, **6**, Part 1, 240 (1984).

14. E. T. CHENG and J. H. HUANG, "A Nuclear Data Library Comparison Study for Tritium Breeding in Helium-Cooled Fusion Blankets," *Trans. Am. Nucl. Soc.*, **46**, 279 (1984).

15. M. A. ABDOU et al., "A Blanket Comparison and Selection Study—Interim Report," ANL/FPP-83-1, Argonne National Laboratory (1983).

16. D. M. DRAKE et al., "Double Differential Beryllium Neutron Cross Sections at Incident Neutron Energies of 5.9, 10.1, and 14.2 MeV," *Nucl. Sci. Eng.*, **63**, 401 (1977).

17. T. K. BASU et al., "Neutron Multiplication Studies in Beryllium for Fusion Reactor Blankets," *Nucl. Sci. Eng.*, **70**, 307 (1979).

18. R. T. HOWERTON and S. T. PERKINS, "Evaluated Neutron Interaction and Gamma-Ray Production Cross Section for ^{9}Be for ENDF/B-IV Mat. No. 1289," UCRL-51603, Lawrence Livermore National Laboratory (1974).

19. R. C. YOUNG and L. STEWART, Los Alamos National Laboratory, Private Communication (1979).

20. F. O. PURSER, Triangle Universities Nuclear Laboratory, Private Communication (1976).

21. N. M. GREEN et al., "AMPX: A Modular Code System for Generating Coupled Multi-Group Neutron and

Gamma Libraries from ENDF/B," ORNL/TM-3706, Oak Ridge National Laboratory (1976).

22. C. R. WEISBIN et al., "Cross Section and Method Uncertainties: The Application of Sensitivity Analysis to Study Their Relationship in Radiation Transport Benchmark Problem," ORNL/TM-4847, Oak Ridge National Laboratory (1975).

23. D. E. BARTINE et al., "Radiation-Transport Cross Section Sensitivity Analysis: A General Approach Illustrated for a Thermonuclear Source in Air," *Nucl. Sci. Eng.*, **55**, 147 (1974).

24. S. A. GERSTL and W. M. STACEY, "A Class of Second-Order Approximate Formulation of Deep Penetration Radiation Transport Problems," *Nucl. Sci. Eng.*, **51**, 339 (1973).

25. F. G. PEREY, "The Data Covariance Files for ENDF/B-V," ORNL/TM-5938, Oak Ridge National Laboratory (1977).

26. "VITAMIN-C: 171 Neutron, 36 Gamma Group Cross Section Library in AMPX Interface Format for Fusion Neutronics Studies," Package DLC-41, Oak Ridge National Laboratory (1978).

27. D. E. BARTINE et al., "SWANLAKE—A Computer Code Utilizing ANISN Transport Calculations for Cross-Section Sensitivity Analysis," ORNL/TM-3809, Oak Ridge National Laboratory (1973).

28. R. G. YOUNG, Los Alamos National Laboratory, Private Communication (1980).

29. P. G. YOUNG, "Evaluation of N+^{7}Li Reactions Using Variance-Covariance Techniques," *Trans. Am. Nucl. Soc.*, **39**, 272 (1981).

30. F. BARRÉ et al., "Fusion Reactor Blanket Neutronic Study in France," *Nucl. Technol./Fusion*, **4**, 799 (1983).

31. M. EMBRECHTS, "Two-Dimensional Cross-Section Sensitivity and Uncertainty Analysis for Fusion Reactor Blankets," LA-9232-T, Los Alamos National Laboratory (1982).

32. T. WU and C. W. MAYNARD, "Higher-Order Sensitivity Theory and Non-Linear Optimization in Fusion Neutronics Studies," UWFDM-402, University of Wisconsin (1981).

33. S. A. W. GERSTL, "Uncertainty Analysis for Secondary Energy Distributions," *Proc. Seminar-Workshop Theory and Application of Sensitivity and Uncertainty Analysis*, Oak Ridge, Tennessee, August 22–24, 1978, ORNL/RSIC-42, Oak Ridge National Laboratory (1979); see also D. W. MUIR, "Applied Nuclear Data Research and Development, April 1–June 30, 1977," LA-6971-PR, Los Alamos National Laboratory (1977).

34. M. Z. YOUSSEF, University of California, Los Angeles, Private Communication (1984).

35. M. Z. YOUSSEF, "Status of Methods, Codes and Applications for Sensitivity and Uncertainty Analysis," *Fusion Technol.*, **8**, 1, Part 2B, 1552 (1985).